Acta Crystallographica Section C
Crystal Structure Communications
ISSN 0108-2701

Lamivudine hemihydrate

Abir Bhattacharya,[a] Bhairab Nath Roy,[b] Girij Pal Singh,[b] Dhananjai Srivastava[b] and Alok K. Mukherjee[a]*

[a]Department of Physics, Jadavpur University, Kolkata 700 032, India, and [b]Lupin Research Park, Lupin Ltd, 46A/47A Nande Village, Mulshi Taluka, Pune 411 042, India
Correspondence e-mail: akm_ju@rediffmail.com

Received 19 May 2010
Accepted 28 May 2010
Online 5 June 2010

A new lamivudine hydrate, namely, *cis*-4-amino-1-(2-hydroxymethyl-1,3-oxathiolan-5-yl)pyrimidin-2(1*H*)-one hemihydrate, $C_8H_{11}N_3O_3S\cdot0.5H_2O$, has been synthesized and structurally characterized by both powder and single-crystal X-ray diffraction studies. The hemihydrate crystallizes in the Sohnke space group $P2_1$, with the asymmetric unit comprising four lamivudine and two water molecules. An extensive network of intermolecular hydrogen bonds involving both lamivudine and solvent water molecules generates a three-dimensional supramolecular architecture. The structural data and crystal packing of the present lamivudine hemihydrate are compared with those of other hydrated and anhydrous forms of lamivudine.

Comment

Lamivudine [*cis*-4-amino-1-(2-hydroxymethyl-1,3-oxathiolan-5-yl)pyrimidin-2(1*H*)-one] is an important pharmaceutical compound with proven antiviral activity (Harris *et al.*, 1997). This reverse transcriptase inhibitor is in clinical use for HIV-infected and hepatitis B-positive patients (Jeong *et al.*, 1993; Hoong *et al.*, 1992). The synthesis and biological evaluation of lamivudine have been studied extensively (Goodyear *et al.*, 2005; Li *et al.*, 2002; Woo *et al.*, 2001; Camplo *et al.*, 1993; Chu *et al.*, 1991). Depending on the solvent employed and the temperature of crystallization, lamivudine is known to exist in two crystal forms (Jozwiakowski *et al.*, 1996). Initial crystallization of lamivudine from solutions in water, methanol or aqueous alcohols resulted in needle-shaped single crystals of the 0.2-hydrate, (I), whereas recrystallization from dry ethanol, *n*-propanol or mixtures of ethanol and less-polar organic solvents produced single crystals of the anhydrous form, (II), as tetragonal bipyramids. A comprehensive analysis of solubility behaviour *versus* temperature and solvent type was carried out in an attempt to reveal the factors responsible for the two different forms of lamivudine (Jozwiakowski *et al.*, 1996). In addition, structural characterization of both the hydrated, (I), and the anhydrous, (II), forms of lamivudine was reported by Harris *et al.* (1997). During our study of the co-crystal forming ability of lamivudine with 5-(cytosin-1-yl)-2-hydroxymethyl-1,3-oxathiolane (Roy *et al.*, 2009), it has been observed that, when slurried in water, both (I) and (II) transform into a new hydrated form, hereinafter referred to as (III). The objective of the present investigation was to characterize this novel lamivudine hemihydrate, (III), and compare its structure with those of (I) and (II) reported earlier (Harris *et al.*, 1997).

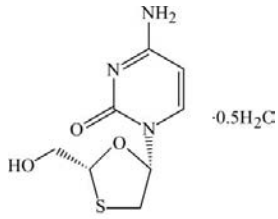

(III)

A scanning electron micrograph (Fig. 1) of single crystals of (III) shows the crystal habit as plates. Comparison of the powder X-ray diffraction (XRD) pattern of (III) with those of (I) and (II) (supplementary Fig. S1) clearly indicates that these are three distinct crystalline phases, and not merely different crystal habits. Although the powder XRD pattern of (III) could be indexed on a monoclinic unit cell, with a = 11.7111 (5), b = 11.2233 (9) and c = 16.2065 (7) Å, and β = 94.678 (3)°, using the program *TREOR* (Werner *et al.*, 1985), our attempts to solve the crystal structure from the powder XRD data were not successful. When the structure of (III) was finally solved *via* single-crystal X-ray analysis, the failure to solve the crystal structure using powder diffraction data was attributed to the presence of four molecules of lamivudine along with two molecules of water in the asymmetric unit. *Ab initio* structure solution of complex molecular crystals with $Z' > 1$ from laboratory X-ray powder diffraction data is still a formidable task (Zhou & Harris, 2009).

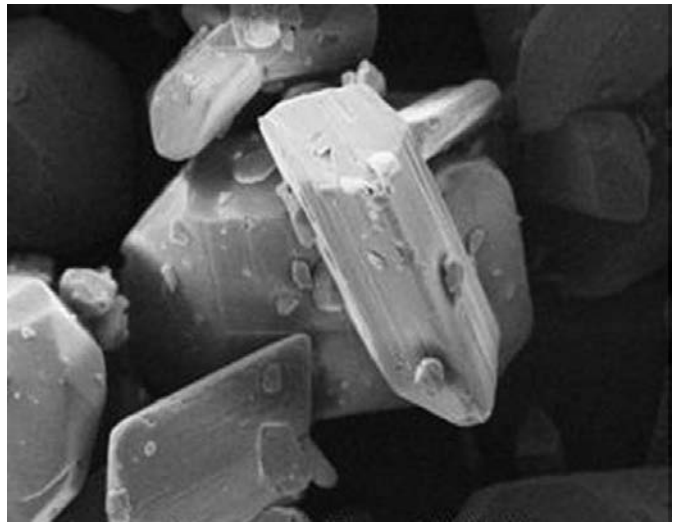

Figure 1
Scanning electron micrograph of lamivudine hemihydrate, (III).

 doi:10.1107/S0108270110020317

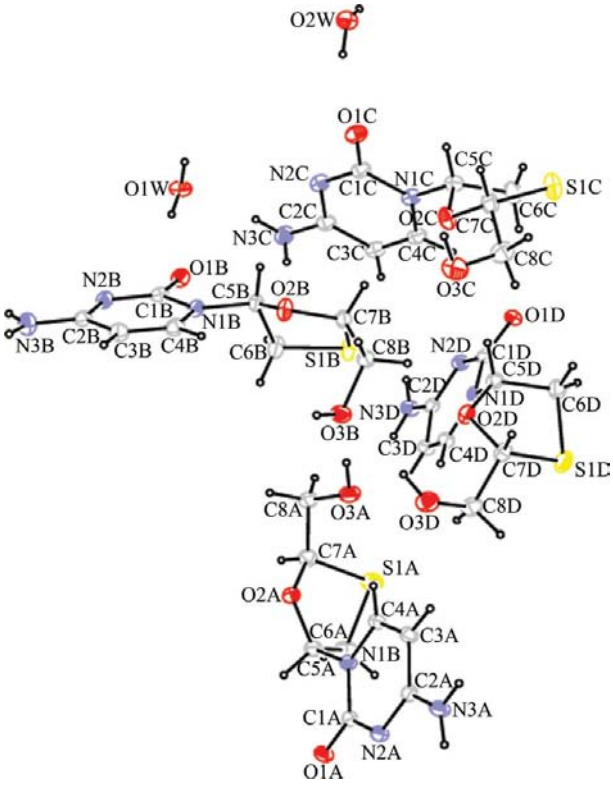

Figure 2
A view of the asymmetric unit of lamivudine hemihydrate, (III), showing the atom-numbering scheme. Displacement ellipsoids are drawn at the 20% probability level and H atoms are shown as small spheres of arbitrary radii.

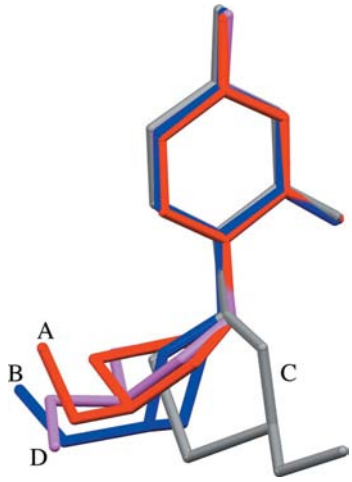

Figure 3
An overlay of the four lamivudine molecules in the asymmetric unit of (III). (Colour code in the electronic version of the paper: molecule *A* red, *B* blue, *C* grey and *D* violet.)

The thermogravimetric (TG) analysis of (III) shows two overlapping steps (supplementary Fig. S2), with a total weight loss of 3.7% (calculated weight loss assuming one-half of a molecule of water for every molecule of lamivudine was 3.8%) due to liberation of solvent water molecules in the temperature range 358–408 K. This is consistent with the stoichiometry (2:1 lamivudine–water) established by the structure analysis of (III). The two-step weight loss in (III) can then be attributed to the two different hydrogen-bonding environments of the water molecules in the crystal structure; atom O1*W* has four neighbouring N/O atoms with intermolecular O1*W*$\cdots$N/O separations < 3.0 Å, whereas the corresponding number for atom O2*W* is only three (see below). The single-step weight loss in the temperature range 393–423 K for form (I), having only one water molecule associated with every five molecules of lamivudine, was about 2% (Harris *et al.*, 1997).

The asymmetric unit of (III) consists of four lamivudine molecules (labelled *A*, *B*, *C* and *D*) and two solvent water molecules (Fig. 2). The structure of (III) is distinctly different from those of the hydrated and anhydrous forms reported in the literature (Harris *et al.*, 1997). Form (I) crystallizes in the orthorhombic system (space group $P2_12_12_1$) with five independent molecules of lamivudine and one of water in the asymmetric unit, whereas form (II) belongs to the tetragonal space group $P4_32_12$ with only one lamivudine molecule in the asymmetric unit. The calculated density of (III), *viz.* 1.504 Mg m^{-3}, which is higher than that of (I) (1.485 Mg m^{-3}) reported by Harris *et al.* (1997) and essentially equal to that of (II) (1.500 Mg m^{-3}), is indicative of the stability of form (III).

The torsion angles (Table 1) about the N1—C5 bond connecting the five- and six-membered rings in (III) indicate that molecules *A*, *B* and *D* have similar conformations to that observed in the anhydrous form, (II) (Harris *et al.*, 1997). The relative orientation of the two heterocyclic rings of molecule *C* in (III) differs from those in molecules *A*, *B* and *D* due to a rotation about the connecting bond. An overlay of the conformations of the four molecules of (III) is shown in Fig. 3. Table 1 also reveals that four molecules (*A*, *B* and one component from each of the disordered molecules *D* and *E*) in the asymmetric unit of (I) assume conformations similar to molecules *A*, *B* and *D* in (III), while the conformations of molecule *C* in (I) and (III) are different. In (II), there is only one solid-state conformation of lamivudine, which is also similar to that of molecules *A*, *B* and *D* of (II) (Table 1).

The pyrimidine rings in the molecules of the asymmetric unit of (III) are essentially planar, with r.m.s. fits of atomic positions in the range 0.01–0.02 Å. The ring-puckering parameters (Cremer & Pople, 1975) indicate that the five-membered S1—C6—C5—O2—C7 heterocyclic ring in each of the four independent lamivudine molecules assumes an envelope conformation; for molecules *A* [q_2 = 0.499 (2) Å and φ_2 = 4.0 (2)°] and *D* [q_2 = 0.495 (2) Å and φ_2 = 7.1 (2)°] the flap atom is S1, whereas in molecules *B* [q_2 = 0.403 (2) Å and φ_2 = 243.9 (2)°] and *C* [q_2 = 0.480 (2) Å and φ_2 = 256.3 (2)°] atom C5 occupies the flap position.

An extensive network of hydrogen bonds (Table 2) connects the molecules of (III) into a supramolecular framework. It is convenient to consider individual substructures generated by the different lamivudine molecules (*A*, *B*, *C* and *D*) in the asymmetric unit through intermolecular hydrogen bonds, and then consider the combination of those substructures to build a three-dimensional framework. The intermolecular hydrogen bonds O3*A*—H3*A*$\cdots$O3*B* and N3*A*—

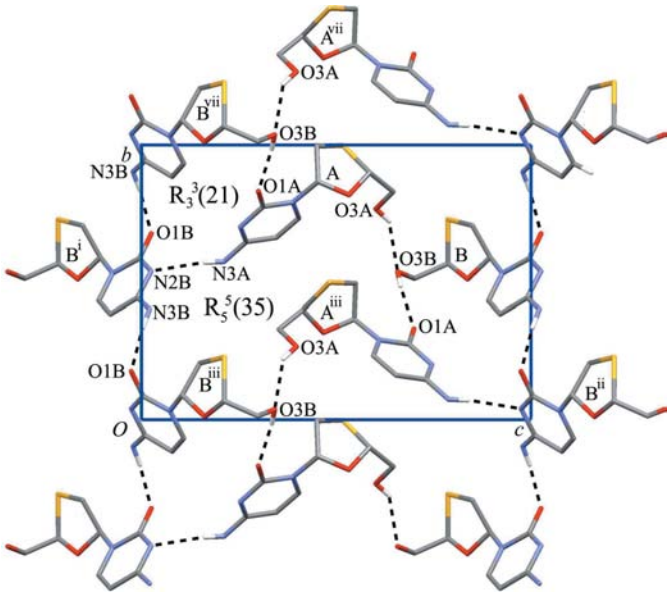

Figure 4
Part of the crystal structure of (III), viewed along the *a* axis, showing the formation of $R_3^3(21)$ and $R_5^5(35)$ rings built from *A* and *B* molecules. For clarity, H atoms not involved in hydrogen bonding have been omitted. (The symmetry codes are as in Table 2.)

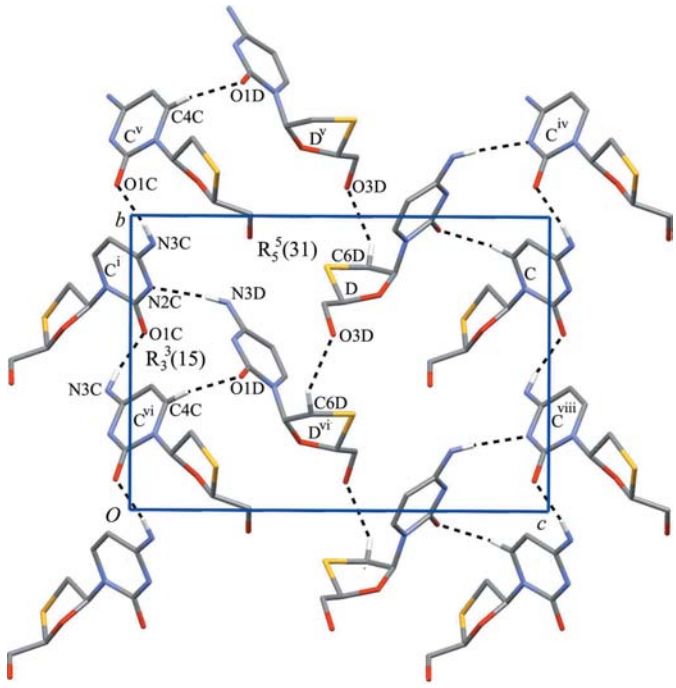

Figure 5
Part of the crystal structure of (III), viewed along the *a* axis, showing the formation of a two-dimensional molecular sheet consisting of *C* and *D* molecules. For clarity, H atoms not involved in hydrogen bonding have been omitted. (The symmetry codes are as in Table 2.)

H3*A*1···N2*B*^{i} (symmetry codes are as in Table 2) generate $C_2^2(20)$ chains (Bernstein *et al.*, 1995) with an ...*ABAB*... sequence propagating along the [001] direction (Fig. 4). The *B* molecules of parallel C_2^2 (20) chains are connected *via* N3*B*—H3*B*2···O1*B*^{ii} hydrogen bonds to form *C*(6) chains running along the [010] direction (Fig. 4). Further linking between adjacent $C_2^2(20)$ chains is provided by O3*B*—H3*B*···O1*A*^{iii} hydrogen bonds, thus generating finite zero-dimensional AB_2 and A_2B_3 building blocks within the structure. In terms of graph-set notation (Etter, 1990), these motifs can be represented as $R_3^3(21)$ and $R_5^5(35)$ rings, which are edge-fused to produce a two-dimensional molecular sheet parallel to the (100) plane (Fig. 4). Similarly, the intermolecular hydrogen bonds N3*C*—H3*C*2···O1*C*^{iv} between adjacent *C* molecules and C6*D*—H6*D*2···O3*D*^{v} between neighbouring *D* molecules produce polymeric *C*(6) chains of ...*CC*... and ...*DD*... sequences along the [010] direction (Fig. 5). Interconnection between parallel *C*(6) chains through hydrogen bonds C4*C*—H4*C*···O1*D* and N3*D*—H3*D*1···N2*C*^{iv} along the [001] direction generates $R_3^3(15)$ and $R_5^5(31)$ rings, which are edge-fused to form another two-dimensional molecular sheet in the (100) plane composed of only *C* and *D* molecules (Fig. 5). Additional reinforcement within each molecular sheet is provided by C6*C*—H6*C*2···O1*D* and C4*B*—H4*B*···O1*A*^{iii} hydrogen bonds. While hydrogen bonds O3*D*—H3*D*···O3*B* and C8*B*—H8*B*1···O2*D* link *B* and *D* molecules to form an $R_2^2(8)$ ring, two N—H···O hydrogen bonds, *i.e.* N3*A*—H3*A*2···O1*D*^{vi} and N3*D*—H3*D*2···O1*A*^{vii}, interconnect the molecular sheets built of *A*/*B* and *C*/*D* molecules along the [100] direction to create a three-dimensional framework. The C3*A*—H3*A*3···O3*D* hydrogen bond merely strengthens this framework.

The formation of the three-dimensional architecture in (III) can be better visualized by considering the two solvent water molecules, which act as hydrogen-bond donors as well as acceptors. Acting as a double donor, atom O1*W* connects molecule types *B* and *D* through O1*W*—H*W*12···O1*B* and O1*W*—H*W*11···N2*D*^{viii} hydrogen bonds, while atom O2*W* links molecules *A* and *C* through O2*W*—H*W*21···O1*C* and O2*W*—H*W*22···N2*A*^{ix} hydrogen bonds. In the remaining three hydrogen bonds, N3*C*—H3*C*1···O1*W*, O3*C*—H3*C*···O1*W*^{viii} and N3*B*—H3*B*2···O2*W*^{x} (Table 2), solvent water molecules O1*W* and O2*W* act as acceptors. The resulting pattern (Fig. 6) crosslinks the *A*/*B* and *C*/*D* layers through chains of molecules in a *B*–O*W*1–*C*–O*W*2–*B*–O*W*1–*C* sequence along the [100] direction, in which molecule *D* is appended to the side of the chain and molecule *A* serves as a linker between adjacent chains. In the graph-set notation, these chains can be represented as $C_4^4(16)[R_3^3(10)][R_3^3(10)]$. Finally, the combination of molecular sheets parallel to the (100) plane (Figs. 4 and 5) and chains along the [100] direction (Fig. 6) results in a three-dimensional architecture in (III).

The role of water molecules in the crystal packing of (III) is thus essentially different from that of the other lamivudine hydrate, (I), reported earlier (Harris *et al.*, 1997). The solvent water molecule in (I) is associated with only one lamivudine molecule (*B*), and there is no close contact (<3.1 Å) of this water molecule to any of the other four lamivudine molecules in the asymmetric unit. Intermolecular hydrogen bonds in (I), with hydroxy O and amine N atoms of different molecules in the asymmetric unit acting as donors to oxo O, pyrimidine N and hydroxy O atoms, connect the five independent lamivu-

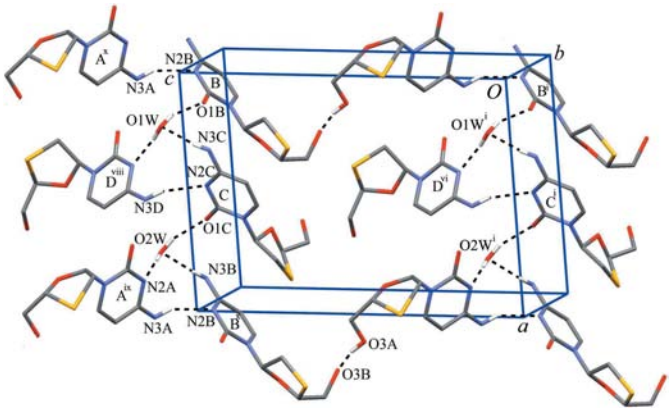

Figure 6
Part of the crystal structure of (III), showing the formation of a $C_4^4(16)[R_3^3(10)][R_3^3(10)]$ synthon *via* crosslinking of *A*/*B* and *C*/*D* layers through solvent water molecules. [Symmetry codes are as in Table 2; in addition: (x) $x, y, z + 1$.]

dine molecules into an *AECDB* sequence. A head-to-head packing of this sequence along the [001] direction is achieved *via* amine–oxo N···O hydrogen bonds between two *B* molecules. The lone solvent water molecule in (I) links these parallel molecular clusters along the [100] direction to form $C_2^2(8)[R_3^3(8)][R_3^3(8)]$ synthons. Further linking of molecules in the [010] direction, where amine N and hydroxy O groups act as donors to oxo O, pyrimidine N and hydroxy O atoms, completes the three-dimensional packing in (I). In the crystal packing of (II), two polymeric chains along the [100] and [010] directions are generated by a single hydroxy–pyrimidine O···N hydrogen bond due to the tetragonal symmetry of the crystal structure. Another chain along the [001] direction is formed by an amine–oxo N···O hydrogen bond, whereas the linking between the chains is provided by amine–oxothiolane N···O hydrogen bonds to form the three-dimensional packing in (II). It is to be noted that the crystal packing in (II) does not exhibit any supramolecular synthon of the type $C_m^m(X)[R_n^n(Y)][R_n^n(Y)]$, as observed in (I) and (III).

Experimental

Lamivudine was synthesized according to the method described by Roy *et al.* (2009). A suspension of lamivudine (25.0 g) in water (75.0 ml) was heated to 318 K over a period of 20 min to give a clear solution. The solution was cooled slowly to 283 K with constant stirring. The colourless precipitate which formed was filtered off, washed with ethanol (2 × 10 ml) and dried *in vacuo* at 318 K for 24 h to give a solid product, lamivudine hemihydrate, (III) [yield 92%; m.p. 450 (1) K]. Single crystals of (III) suitable for X-ray structure analysis were obtained by slow evaporation from an aqueous solution.

X-ray powder diffraction data for (III) were recorded with a Philips X'pert system over an angular range $2\theta = 3.5$–40° using a step size of 0.008° and a counting time of 24.765 s per step.

Thermogravimetric (TG) data were recorded with a Perkin–Elmer Pyris 1 thermobalance at a heating rate of 10 K min^{-1}. The scanning electron microscopic analysis was carried out on a Leica Stereoscan 440 instrument.

Table 1
Selected torsion angles (°) in lamivudine forms (I)–(III).

	Molecule	C1—N1—C5—O2	C1—N1—C5—C6	C4—N1—C5—O2	C4—N1—C5—C6
(III)	*A*	145.45 (14)	−93.70 (17)	−31.7 (2)	89.18 (19)
	B	169.88 (13)	−72.51 (19)	−10.7 (2)	106.88 (19)
	C	86.47 (17)	−155.38 (16)	−89.05 (19)	29.1 (2)
	D	160.53 (13)	−78.45 (17)	−15.8 (2)	105.22 (18)
(I)	*A*	151.9 (5)	−87.2 (6)	−31.7 (7)	89.2 (7)
	B	158.3 (5)	−82.6 (6)	−21.6 (7)	97.5 (6)
	C	109.3 (6)	−130.2 (6)	−72.1 (7)	48.4 (8)
	D	140.6 (5)	−88.9 (12)	−43.0 (7)	87.5 (12)
	D′	140.6 (5)	−107.8 (9)	−43.0 (7)	68.6 (9)
	E	143.8 (5)	−75.4 (9)	−32.0 (8)	108.8 (8)
	E′	143.8 (5)	−113.6 (7)	−32.0 (8)	70.6 (8)
(II)		152.1 (4)	−84.8 (5)	−29.8 (6)	93.3 (5)

Crystal data

$C_8H_{11}N_3O_3S{\cdot}0.5H_2O$
$M_r = 238.27$
Monoclinic, $P2_1$
$a = 11.5729$ (4) Å
$b = 11.2385$ (4) Å
$c = 16.0232$ (6) Å
$\beta = 94.329$ (1)°
$V = 2078.06$ (13) Å^3
$Z = 8$
Mo $K\alpha$ radiation
$\mu = 0.31$ mm^{-1}
$T = 120$ K
0.35 × 0.25 × 0.08 mm

Data collection

Bruker Kappa APEXII CCD area-detector diffractometer
Absorption correction: multi-scan (*SADABS*; Bruker, 2001)
$T_{min} = 0.931$, $T_{max} = 0.975$
28475 measured reflections
9309 independent reflections
8846 reflections with $I > 2\sigma(I)$
$R_{int} = 0.027$

Refinement

$R[F^2 > 2\sigma(F^2)] = 0.028$
$wR(F^2) = 0.071$
$S = 1.04$
9309 reflections
748 parameters
3 restraints
H atoms treated by a mixture of independent and constrained refinement
$\Delta\rho_{max} = 0.43$ e Å^{-3}
$\Delta\rho_{min} = -0.24$ e Å^{-3}
Absolute structure: Flack (1983), with 4338 Friedel pairs
Flack parameter: 0.00 (3)

All H atoms were located in difference Fourier maps and refined with isotropic displacement parameters, except for atoms H8*C*2 and H4*D*, for which the C—H distances were restrained to 0.96 (2) Å. The absolute configuration of (III) was established from anomalous dispersion effects in the measured diffraction data.

Data collection: *APEX2* (Bruker, 2007); cell refinement: *APEX2* and *SAINT* (Bruker, 2007); data reduction: *SAINT* and *XPREP* (Bruker, 2007); program(s) used to solve structure: *SHELXS97* (Sheldrick, 2008); program(s) used to refine structure: *SHELXL97* (Sheldrick, 2008); molecular graphics: *ORTEP-3 for Windows* (Farrugia, 1997) and *Mercury* (Macrae *et al.*, 2006); software used to prepare material for publication: *PLATON* (Spek, 2009).

AB thanks the University Grants Commission, India, for a research fellowship. The authors thank Dr P. R. Upadhayay, Analytical Development, Lupin Research Park, Pune, India, for providing analytical support, and Dr Vishvas D. Patil, Intellectual Property Cell, Lupin Research Park, Pune, India, for the literature search. The authors acknowledge the DST-funded National Single-Crystal X-ray Diffraction Facility at the Department of Inorganic Chemistry, IACS, India, and Mr S. Chakraborty, Bruker AXS, India, for data collection.

Table 2
Hydrogen-bond geometry (Å, °).

D—H···A	D—H	H···A	D···A	D—H···A
O3A—H3A···O3B	0.83 (3)	2.22 (3)	2.9368 (19)	144 (3)
N3A—H3A1···N2B^{i}	0.84 (2)	2.25 (3)	3.012 (2)	151 (2)
N3B—H3B2···O1B^{ii}	0.87 (3)	1.98 (3)	2.851 (2)	173 (2)
O3B—H3B···O1A^{iii}	0.73 (3)	2.05 (3)	2.7717 (19)	168 (3)
N3C—H3C2···O1C^{iv}	0.87 (3)	1.96 (3)	2.826 (2)	169 (2)
C6D—H6D2···O3D^{v}	0.97 (2)	2.43 (2)	3.165 (2)	131.8 (16)
C4C—H4C···O1D	0.98 (2)	2.24 (2)	3.150 (2)	155.2 (19)
N3D—H3D1···N2C^{iv}	0.87 (2)	2.20 (2)	3.031 (2)	162 (2)
C6C—H6C2···O1D	0.97 (2)	2.42 (2)	3.368 (2)	167.6 (18)
C4B—H4B···O1A^{iii}	0.93 (2)	2.48 (2)	3.338 (2)	155.3 (17)
O3D—H3D···O3B	0.88 (3)	2.04 (3)	2.903 (2)	165 (3)
C8B—H8B1···O2D	0.98 (2)	2.44 (2)	3.208 (2)	134.3 (17)
N3A—H3A2···O1D^{vi}	0.82 (2)	2.08 (2)	2.896 (2)	170 (2)
N3D—H3D2···O1A^{vii}	0.86 (2)	2.12 (3)	2.958 (2)	164 (2)
C3A—H3A3···O3D	0.90 (2)	2.49 (2)	3.145 (2)	129.7 (17)
O1W—H12W···O1B	0.81 (3)	1.98 (3)	2.7411 (18)	157 (3)
O1W—H11W···N2D^{viii}	0.82 (3)	1.97 (3)	2.781 (2)	172 (3)
O2W—H21W···O1C	0.82 (3)	1.96 (3)	2.7546 (19)	161 (3)
O2W—H22W···N2A^{ix}	0.79 (3)	2.18 (3)	2.966 (2)	177 (3)
N3C—H3C1···O1W	0.85 (2)	2.10 (3)	2.944 (2)	173 (2)
O3C—H3C···O1W^{viii}	0.91 (3)	1.80 (3)	2.698 (2)	166 (3)
N3B—H3B1···O2W^{x}	0.83 (2)	2.11 (2)	2.933 (2)	174 (2)

Symmetry codes: (i) $x, y, z-1$; (ii) $-x, y-\frac{1}{2}, -z+2$; (iii) $-x, y-\frac{1}{2}, -z+1$; (iv) $-x+1, y+\frac{1}{2}, -z+2$; (v) $-x+1, y+\frac{1}{2}, -z+1$; (vi) $-x+1, y-\frac{1}{2}, -z+1$; (vii) $-x, y+\frac{1}{2}, -z+1$; (viii) $-x+1, y-\frac{1}{2}, -z+2$; (ix) $x+1, y, z+1$; (x) $x-1, y, z$.

Supplementary data for this paper are available from the IUCr electronic archives (Reference: LN3144). Services for accessing these data are described at the back of the journal.

References

Bernstein, J., Davis, R. E., Shimoni, L. & Chang, N.-L. (1995). *Angew. Chem. Int. Ed. Engl.* **34**, 1555–1573.
Bruker (2001). *SADABS*. Bruker AXS Inc., Madison, Wisconsin, USA.
Bruker (2007). *APEX2*, *SAINT* and *XPREP*. Bruker AXS Inc., Madison, Wisconsin, USA.
Camplo, M., Faury, P., Charvet, A.-S., Lederer, F., Chermann, J.-C. & Kraus, J.-L. (1993). *Nucleosides Nucleotides*, **12**, 631–641.
Chu, C. K., Beach, J. W., Jeong, L. S., Choi, B. G., Comer, F. I., Alves, A. J. & Schinazi, R. F. (1991). *J. Org. Chem.* **56**, 6503–6505.
Cremer, D. & Pople, J. A. (1975). *J. Am. Chem. Soc.* **97**, 1354–1358.
Etter, M. C. (1990). *Acc. Chem. Res.* **23**, 120–126.
Farrugia, L. J. (1997). *J. Appl. Cryst.* **30**, 565.
Flack, H. D. (1983). *Acta Cryst.* A**39**, 876–881.
Goodyear, M., Hill, M., West, J. & Whitehead, A. (2005). *Tetrahedron Lett.* **46**, 8535–8538.
Harris, R. K., Yeung, R. R., Lamont, R., Lancaster, R., Lynn, S. & Staniforth, S. J. (1997). *J. Chem. Soc. Perkin Trans. 2*, pp. 2653–2659.
Hoong, L., Strange, L., Liotta, D., Koszalka, G., Burns, C. & Schinazi, R. (1992). *J. Org. Chem.* **57**, 5563–5565.
Jeong, L., Schinazi, R., Beach, J., Kim, H., Nampalli, S., Shanmuganathan, K., Alves, A., McMillan, A., Chu, C. & Mathis, R. (1993). *J. Med. Chem.* **36**, 181–195.
Jozwiakowski, M. J., Nguyen, N.-A. T., Sisco, J. M. & Spancake, C. W. (1996). *J. Pharm. Sci.* **85**, 193–199.
Li, J., Gao, L. & Ding, M. (2002). *Synth. Commun.* **32**, 2355–2359.
Macrae, C. F., Edgington, P. R., McCabe, P., Pidcock, E., Shields, G. P., Taylor, R., Towler, M. & van de Streek, J. (2006). *J. Appl. Cryst.* **39**, 453–457.
Roy, B. N., Singh, G. P., Srivastava, D., Jadhav, H. S., Saini, M. B. & Aher, U. P. (2009). *Org. Process Res. Dev.* **13**, 450–455.
Sheldrick, G. M. (2008). *Acta Cryst.* A**64**, 112–122.
Spek, A. L. (2009). *Acta Cryst.* D**65**, 148–155.
Werner, P.-E., Eriksson, L. & Westdahl, M. (1985). *J. Appl. Cryst.* **18**, 367–370.
Woo, J., Shin, H., Kim, T., Ghim, S., Jeong, L., Kim, J. & Song, B. (2001). *Biotechnol. Lett.* **23**, 131–135.
Zhou, Z. & Harris, K. D. M. (2009). *Comput. Mater. Sci.* **45**, 118–121.